Current Optics and Photonics
Vol. 1, No. 1, February 2017, pp. 45-50

ISSN: 2508-7266(Print) / ISSN: 2508-7274(Online)
DOI: https://doi.org/10.3807/COPP.2017.1.1.045

Operating Voltage of Optical Instruments based on Polymer-dispersed Liquid Crystal for Inspecting Transparent Electrodes

Sunggu Yeo, Yonghwan Oh, and Ji-Hoon Lee*

Division of Electronics Engineering, Chonbuk National University, Jeonbuk 54896, Korea

(Received September 26, 2016 : revised December 8, 2016 : accepted December 14, 2016)

Optical instruments based on polymer-dispersed liquid crystal (PDLC) have been used to inspect transparent electrodes. Generally the operating voltage of an inspection instrument using PDLC is very high, over 300 V, reducing its lifetime and reliability. The operating-voltage issue becomes more serious in the inspection of touch-screen panel (TSP) electrodes, due to the bezel structure protruding over the electrodes. We have theoretically calculated the parameters affecting the operating voltage as a function of the distance between the TSP and the PDLC, the thickness, and the dielectric constant of the sublayers when the inspection module was away from the TSP electrodes. We have experimentally verified the results, and have proposed a way to reduce the operating voltage by substituting a plastic substrate film with a hard coating layer of smaller thickness and higher dielectric constant.

Keywords : Optical inspection, Transparent electrode, Polymer-dispersed liquid crystal, Scattering
OCIS codes : (163.3710) Liquid crystals; (120.4630) Optical inspection; (120.2040) Displays

I. INTRODUCTION

Touch-screen panels (TSP) are widely used in mobile electronic devices such as smart phones and tablet computers. Various kinds of TSP modules using different principles of operation have been developed. Among them, methods sensing the change in resistance or capacitance are commonly used these days [1-3]. In spite of the growth in TSP-embedded products, the TSP market has become very crowded these days; hence the inspection and repair of defective TSP electrodes is essential for cost reduction. For display applications, the TSP electrodes required to sense a change in impedance should be transparent. For this reason, inspection of TSP electrodes by the naked eye is difficult. Although inspection by electrical probe tip can be used, it takes a very long time to check the entire area of a TSP panel, due to its narrow probe area [4, 5].

As another means to inspect TSP electrodes, polymer-dispersed liquid crystal (PDLC) can be used [6-11]. The PDLC is a switchable film in which liquid crystal (LC) droplets are dispersed in a polymer matrix (Fig. 1). In the zero-field state, the LC droplets are randomly oriented and the incident light is scattered due to mismatch of the refractive indices of LC (n_{LC}) and polymer (n_p) (Fig. 1(a)). In an applied electric field, the LC molecules are vertically aligned along the field and n_{LC} matches n_p, resulting in the transmission of light (Fig. 1(b)).

Figure 2 shows the operation principle for TSP electrode inspection using the PDLC. The proposed PDLC inspection module is composed of an indium tin oxide (ITO)-covered

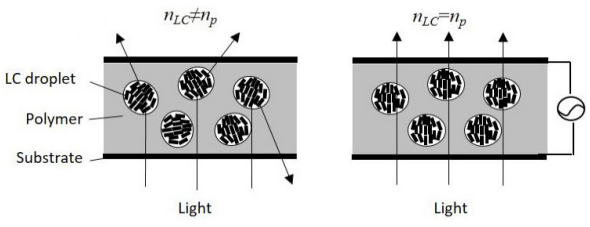

FIG. 1. Schematic illustration of the principle of operation for a PDLC in (a) the scattering state and (b) the transparent state.

*Corresponding author: jihoonlee@jbnu.ac.kr

Color versions of one or more of the figures in this paper are available online.

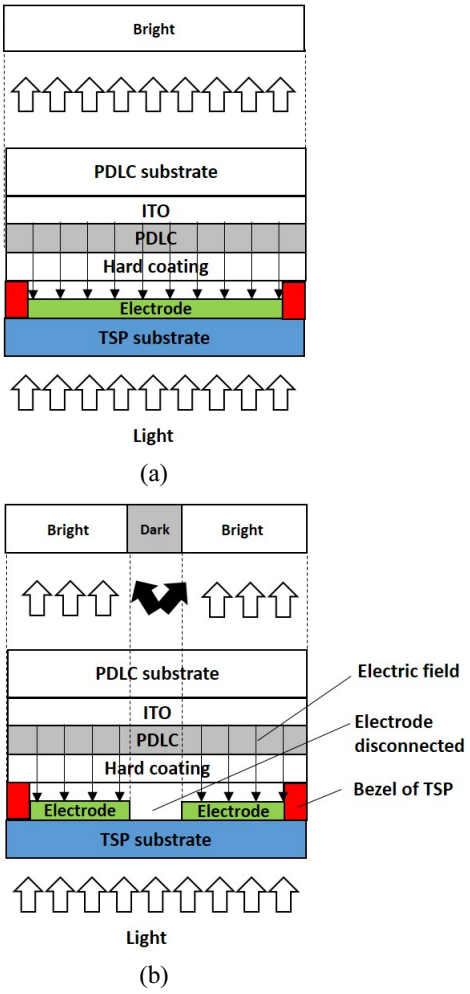

FIG. 2. Operation principle for TSP electrode inspection using PDLC. Light propagation through the TSP electrode, (a) without a disconnection and (b) with a disconnection.

glass substrate, upon which layers of PDLC and a hard coating (HC) are consecutively stacked (Fig. 2). For the inspection, an electric field is applied between the ITO layer in the PDLC module and the TSP electrodes. With the electric field applied, the probe light can pass through the PDLC layer without scattering, provided that no defective point (*e.g.* a disconnected electrode) is on the TSP module (Fig. 2(a)). On the other hand, if the TSP electrode is disconnected, the electric field is not applied across the PDLC above the disconnected point, and consequently the probe light is scattered from the defect point (Fig. 2(b)). Thus the connected area and the disconnected area respectively look bright and dark, which can be distinguished easily by the naked eye.

Although there have been several reports about the application of PDLC to the inspection module [12, 13], the high operating voltage of the PDLC has not been completely resolved. Generally, the switching voltage needed to obtain the transparent state of the PDLC is very high: over 30 V, when the PDLC is sandwiched between ITO glasses with a cell gap of 10 μm. Moreover, the PDLC inspection module should be separated from the TSP electrode, typically over 10 μm, due to the bezel structure protruding above the electrode plane (see Fig. 2). Consequently, the operating voltage of the typical PDLC inspection module is over 300 V. If the capacitance of the TSP is too large, such a high operating voltage cannot be supplied by a power source. In addition, the high operating voltage often reduces the lifetime and reliability of the inspection module and the object of inspection.

The purpose of this paper can be summarized as follows. First, we theoretically calculate the parameters affecting the operating voltage of the inspection instrument. Although there is previous literature about calculating the operating voltage of a PDLC, there the PDLC module was in contact with the transparent electrode [12, 13]. However, as described above, the TSP electrodes should be away from the PDLC module, due to the bezel structure at the boundary of the TSP (Fig. 2). Thus, we derived a more general expression for the operating voltage of the PDLC inspection module, considering the distance between the TSP and the PDLC module.

As the second purpose of this paper, we propose a method to reduce the operating voltage of the TSP inspection module. As described above, the operating voltage of a PDLC module that is separated from the TSP is much increased, compared to the contact case. To reduce the voltage, we replace the top substrate film with a HC layer. The HC layer has a smaller thickness as well as a greater dielectric constant compared to the plastic film, and the operating voltage can be effectively reduced. We also calculate the operating voltage of the PDLC module as a function of the thicknesses and dielectric constants of the sublayers.

II. METHODS

A commercial nematic LC mixture (ZKC-5109XX, JNC) was mixed with a UV-reactive monomer mixture (NOA65, Norland products) at a weight ratio of 6:4. The LC mixture has a large optical birefringence Δn = 0.25 at a wavelength of 589 nm, and $\Delta\varepsilon$ = 20.2 at an electric field of 1 kHz. The extraordinary and ordinary refractive indices of the ZKC-5109XX are 1.771 and 1.521 respectively. The LC-monomer mixture was stirred at 80°C for 10 minutes and cooled to room temperature at a cooling rate of 5°C/min. The mixture was then spin-coated on the ITO glass at 1500 rpm for 20 seconds. The coated substrate was exposed to UV light with an intensity of 30 mW/cm^2 for 10 minutes with a nitrogen-gas purge. Then, a commercial HC layer (SE8110, fotopolymer) was overcoated on the PDLC layer at 3000 rpm for 20 seconds. The HC layer was also exposed to the UV light under the same conditions above. Figure 3 shows the reflective optical microscopy image of the fabricated PDLC module. The HC layer is well separated from the

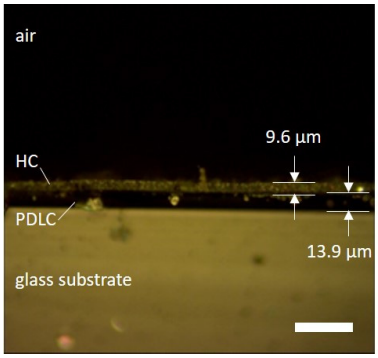

FIG. 3. Cross-sectional image of the PDLC module. The HC layer is overcoated on the PDLC layer. Scale bar corresponds to 50 μm.

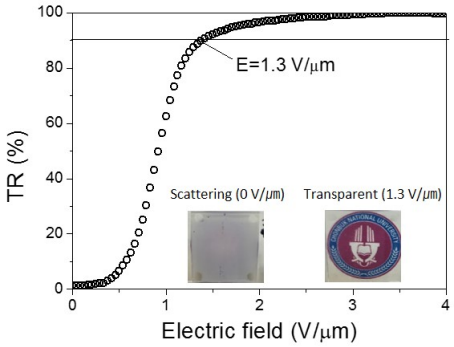

FIG. 4. Normalized transmittance (TR) versus applied voltage for the PDLC sandwiched between ITO glass substrates. The insets show a sample image in the scattering (0 V/μm) and transparent (1.3 V/μm) states.

PDLC layer. The thicknesses of the HC and the PDLC layers were 9.6 and 13.9 μm respectively. The relative dielectric constants of the HC and PDLC layers were ε_{rh} = 4.98 and ε_{rp} = 6.57, measured from the capacitance value with a LCR meter (ZSM2376, NF) at 1 kHz [14, 15].

For the inspection test, we used a commercial capacitive-type TSP module (ER-TPC043-2, Eastrising). The column and row ITO electrodes are orthogonally crossed beneath and under a glass substrate in this TSP module. The PDLC module was placed on the TSP module, and a 1 kHz square bipolar voltage generated from a function generator (33210, Agilent) was applied through a voltage amplifier (TREK2210, TREK). The optical image during inspection was obtained using a polarizing optical microscope (50iPol, Olympus).

III. RESULTS and DISCUSSION

Before investigating the switching property of the PDLC module, we first measured the basic switching property of the PDLC that was sandwiched between two ITO substrates. In this case, the PDLC layer is contacted between the ITO layers. Figure 4 shows the normalized transmittance (TR) of the PDLC versus applied electric field. Here "normalized TR" means the transmitted intensity normalized to the maximum TR value with a 4.0 V/μm electric field applied. The maximum intensity of the transmitted light with a 4.0 V/μm electric field applied was about 80% of the input beam intensity. The normalized TR was minimal in the zero-field state and gradually increased with increasing electric field. The electric field allowing 90% of the normalized TR was 1.3 V/μm. The insets of Fig. 4 show the PDLC sample on paper; one can easily distinguish the scattering state (0 V/μm) and the transparent state (1.3 V/μm). The contrast ratio for the PDLC sample checked from Fig. 4 was 83:1, which can be recognized easily by the naked eye.

The arrangement of the PDLC inspection module and TSP electrodes is illustrated in Fig. 5. From the boundary condition, the electric field applied across the air gap (E_1)

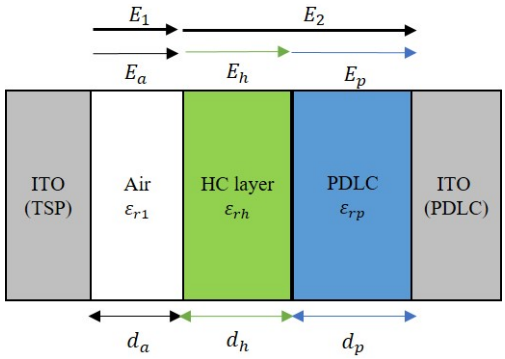

FIG. 5. Schematic illustration of the modeled structure of the PDLC inspection module.

and that across the dielectric layers including the HC and the PDLC layers (E_2) can be related as

$$\varepsilon_{r1}E_1 = \varepsilon_{r2}E_2 \tag{1}$$

where ε_{r1} and ε_{r2} are the relative dielectric constants of the air and the HC-PDLC layer respectively [16, 17]. Integrating the field from the TSP electrode to the other ITO should yield the applied voltage V from the external power source:

$$E_1 d_a + E_2(d_h + d_p) = V \tag{2}$$

where d_a, d_h, and d_p are the thicknesses of the air gap, HC, and PDLC layers respectively. Eliminating E_1 from Eqs. (1) and (2), E_2 is given by

$$E_2 = \frac{\varepsilon_{r1}}{\varepsilon_{r2} - \frac{(d_h + d_p)}{(d_a + d_h + d_p)}(\varepsilon_{r2} - \varepsilon_{r1})}\left(\frac{V}{d_a + d_h + d_p}\right) \tag{3}$$

Applying the boundary condition at the interface between the HC and the PDLC layer, the electric field applied across the HC (E_h) and PDLC (E_p) layers can be related as

$$\varepsilon_{rh}E_h = \varepsilon_{rp}E_p \tag{4}$$

$$E_h + E_p = E_2 \tag{5}$$

where ε_{rh} and ε_{rp} are the relative dielectric constants of the HC and PDLC layers respectively [16, 17]. Eliminating E_h in Eqs. (4) and (5), E_p is given by

$$E_p = E_2 - E_h = \frac{E_2}{\frac{\varepsilon_{rp}}{\varepsilon_{rh}}+1} \tag{6}$$

Considering a capacitor in which the HC and PDLC layers are serially connected between two electrodes, the capacitance C_2 is given by

$$C_2 = \frac{\varepsilon_o \varepsilon_{r2} A}{d_s + d_p} \tag{7}$$

where A is the area of the capacitor. Eq. (7) also equals

$$C_2 = \frac{C_h C_p}{C_h + C_p} = \frac{\varepsilon_0 \varepsilon_{rh}\frac{A}{d_s}\varepsilon_0 \varepsilon_{rp}\frac{A}{d_p}}{\varepsilon_0 \varepsilon_{rh}\frac{A}{d_s} + \varepsilon_0 \varepsilon_{rp}\frac{A}{d_p}} \tag{8}$$

Manipulating Eqs. (7) and (8), ε_{r2} can be written as,

$$\varepsilon_{r2} = \frac{\frac{\varepsilon_{rh}}{d_h}\frac{\varepsilon_{rp}}{d_p}}{\frac{\varepsilon_{rh}}{d_h} + \frac{\varepsilon_{rp}}{d_p}}(d_h + d_p) \tag{9}$$

Substituting the result of Eq. (9) in Eqs. (3) and (6), we finally obtain E_p as a function of the experimental parameters:

$$E_p = \frac{1}{(d_h + d_p)\left(d_a \frac{\varepsilon_{rh}\varepsilon_{rp}}{\varepsilon_{rh}d_p + \varepsilon_{rp}d_h} + 1\right)} \frac{1}{\left(\frac{\varepsilon_{rp}}{\varepsilon_{rh}} + 1\right)} V \tag{10}$$

Figure 6 shows the calculated E_p value versus applied voltage V using Eq. (10). Figure 6(a) shows the calculated result for E_p with d_a varied. For this calculation, d_h and d_p were set to be 10 μm and experimentally measured ε_{rh} = 4.98 and ε_{rp} = 6.57 were substituted. E_p diminished rapidly with increasing d_a. The electric field to obtain 90% TR was 1.3 V/μm in Fig. 2; thus d_a should be smaller than 20 μm to apply an electric field over 1.3 V/μm, provided that the applied voltage is less than 400 V. Figure 6(b) depicts the E_p value with d_h varied. In this calculation, d_a and d_p were set to be 10 μm. It is observed that an E_p over 1.3 V/μm can be obtained, provided that d_h is smaller than 30 μm for an applied voltage of 300 V. Figure 6(c) shows the E_p value with d_p varied. It is observed that an E_p over 1.3 V/μm can be obtained, provided that d_p is smaller than 30 μm for a 300 V external field. It is also concluded that the dependence of E_p on d_a was more significant than that on d_h or d_p. This is due to the higher dielectric permittivities of the HC and PDLC layers (ε_{rh} = 4.98 and ε_{rp} = 6.57) than that of the air (ε_{r1} = 1), which is also consistent with Eq. (10).

Figure 7 shows the calculated E_p value versus applied voltage V with ε_{rh} and ε_{rp} varied. We used sublayer thicknesses d_a = 10 μm, d_h = 9.6 μm, and d_p = 13.9 μm, which were measured in Fig. 3. E_p increased with increasing ε_{rh} (Fig. 7(a)), while E_p decreased with increasing ε_{rp} (Fig. 7(b)). The dependence of E_p on ε_{rp} was greater than on ε_{rh}, due to d_p being thicker than d_h. It is observed that an E_p over 1.3 V/μm can be obtained, provided that ε_{rh} is greater than 2.98 with 260 V applied (Fig. 7(a)). The same E_p can be obtained using a PDLC with ε_{rp} smaller than 8.57 with 260 V applied (Fig. 7(b)). Thus, it is favorable to use a HC layer with a high ε_{rh} value and a PDLC with a low ε_{rp}, to reduce the operating voltage of the inspection module. Doping a small amount of nanoparticles with high dielectric constant into the HC layer could be a useful solution for reducing the operating voltage.

To confirm the validity of the theoretical calculations, we fabricated the PDLC module and investigated the operating voltage using the TSP electrodes. Figure 8 shows the normalized TR of the PDLC-TSP module versus applied voltage. A square voltage at 1 kHz was applied across the PDLC,

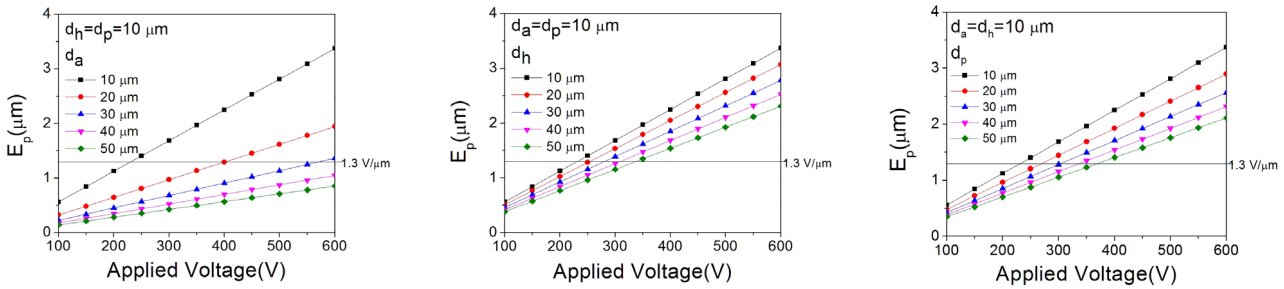

FIG. 6. Calculated electric field applied across the PDLC layer versus applied voltage from the power supply. (a) d_a, (b) d_h, and (c) d_p were varied in the calculation. ε_{r1} = 1, ε_{rh} = 4.98, and ε_{rp} = 6.57 in this calculation.

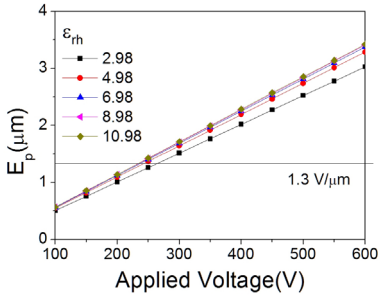

(a)

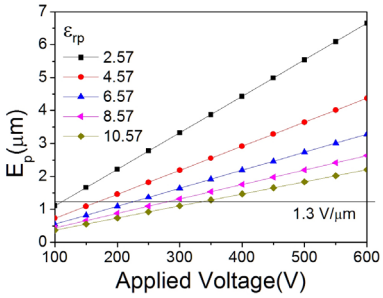

(b)

FIG. 7. Calculated electric field applied across the PDLC layer versus applied voltage from the power supply. (a) ε_{rh} and (b) ε_{rp} were varied in the calculation. d_a = 10 μm, d_h = 9.6 μm, and d_p = 13.9 μm in this calculation.

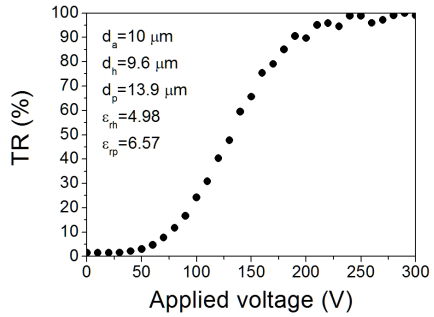

FIG. 8. Normalized TR versus applied voltage for a PDLC module 10 μm away from the TSP module.

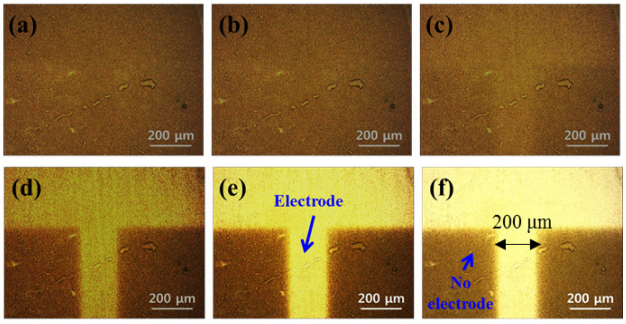

FIG. 9. Transmissive optical image of the TSP-PDLC inspection module with (a) 0, (b) 50, (c) 100, (d) 150, (e) 200, and (f) 250 V applied. The width of the electrode is 200 μm.

the HC, and the air gap. The measurement conditions were d_a = 10 μm, d_h = 9.6 μm, and d_p = 13.9 μm. ε_{rh} and ε_{rp} were 4.98 and 6.57 respectively. From the theoretical calculation (blue triangles in Fig. 7(b)), the electric field required for 90% TR was 230 V; the experimental value for 90% TR in Fig. 8 was about 200 V, which was even smaller than the theoretical value. The smaller switching voltage of the experimental result seems to be related to some differences in the LC orientation and the polymer matrix structure. The theoretical value was estimated based on the TR versus voltage data for the sandwich type PDLC cell (Fig. 4), but the experimental value in Fig. 8 was measured for a PDLC cell that was fabricated without one of the substrates. The different surface condition may result in different morphology of the polymers, affecting on the switching voltage [10, 11].

Figure 9 shows the transmissive optical microscopy image of the TSP-PDLC inspection module with various voltages applied. For the measurement, d_a was maintained at 10 μm. According to the experimental setup in Fig. 2, the zone where the electrode is connected becomes brighter with increasing electric field, while the zone with a disconnected electrode remains dark, due to scattering of the light. With increasing electric field between the electrodes of the PDLC and those of the TSP, the electrode zone becomes brighter and the extinction gets more vivid. The extinction was nearly saturated when the applied voltage was over 200 V, which coincides with the result of Fig. 8. We should note that the operating voltage of the PDLC module was about 310 V when polyethylene terephthalate (PET) of thickness 20 μm and dielectric constant ε_r = 3.2 was used as the substrate film. Thus, the operating voltage can be significantly reduced by substituting the typical PET film with an HC layer of smaller thickness and greater dielectric constant. The width of the electrode in Fig. 9 was 200 μm. The electrode zone could be directly distinguished, provided the width of the electrode was over 5.0 μm. When the width of the electrode was smaller than 5.0 μm, the electrode zone was difficult to distinguish, due to the scattering of light and the fringe-field effect [18, 19].

IV. CONCLUSION

To summarize, we theoretically calculated the operation voltage of a PDLC module for inspecting TSP electrodes. Considering the bezel structure of the TSP module, we derived a more general expression for the operating voltage when the PDLC module was separated from the TSP electrodes. We investigated the effects of changing various parameters, such as the distance between the TSP and the PDLC, the thicknesses of the sublayers, and the dielectric constants of the materials used. We experimentally confirmed that the calculated operating voltage was a good approximation to the experimental value. In addition, the operating voltage of the inspection module could be decreased from

310 to 200 V by substituting one substrate film with an HC layer of smaller thickness and greater dielectric constant. The suggested results will be helpful for the design and development of transparent-electrode inspection systems.

ACKNOWLEDGMENT

This research was supported by small and medium business administration (SMBA, S2295383), BK21 plus project, and national research foundation (NRF, 2016R1A2B4010361).

REFERENCES

1. J. A. Pickering, "A highly area-efficient controller for capacitive touch screen panel systems," Int. J. Man. Mach. Stud. **25**, 249-269 (1986).
2. T.-H. Hwang, W.-H. Cui, I.-S. Yang, and O.-K. Kwon, "A highly area-efficient controller for capacitive touch screen panel systems," IEEE Trans. Cons. Elec. **56**, 1115-1122 (2010).
3. H.-K. Kim, S. Lee, and K.-S. Yun, "Capacitive tactile sensor array for touch screen application," Sensor. Actuat. A: Phys. **165**, 2-7, (2011).
4. K. Kinameri, C. Munakata, and K. Mayama, "A scanning photon microscope for non-destructive observations of crystal defect and interface trap distributions in silicon wavers," J. Phys. E: Sci. Instrum. **21**, 91-97 (1988)
5. M. Koerdel, F. Alatas, A. Schick, K. Kragler, R. L. Weisfield, S. J. Rupitsch, and R. Lerch, IEEE, "Contactless inspection of flat-panel displays and detector panels by capacitive coupling," Trans. Elec. Dev. **58**, 3453-3462 (2011).
6. J. L. West, "Phase-separation of liquid-crystals in polymers," Mol. Cryst. Liq. Cryst. **157**, 427-441 (1988).
7. J. W. Doane, A. Golemme, J. L. West, J. B. Whitehead Jr., and B.-G. Wu, "Polymer dispersed liquid crystals for display application," Mol. Cryst. Liq. Cryst. **165**, 511-532 (1988).
8. R. Ondris-Crawford, E. P. Boyko, B. G. Wagner, J. H. Erdmann, S. Zumer, and J. W. Doane, "Microscope textures of nematic droplets in polymer dispersed liquid crystals," J. Appl. Phys. **69**, 6380-6386 (1991).
9. D. K. Yang, J. L. West, L. C. Chien, and J. W. Doane, "Control of reflectivity and bistability in displays using cholesteric liquid crystals," J. Appl. Phys. **76**, 1331-1333 (1994).
10. M. J. Coles, C. Carboni, and H. J. Coles, "A highly bistable fast-shear aligned polymer dispersed ferroelectric liquid crystal device," Liq. Cryst. **26**, 679-684 (1999).
11. P. J. Collings and J. S. Patel, Handbook of Liquid Crystal Research, (Oxford University Express, 1997) Chap. 9.
12. X. Chen, "New-Generation electro-optic modulator for TFT array inspection," SID Symposium Digest of Technical Papers, 1792-1795 (2005).
13. C.-H. Chan, Y.-T. Zou, T.-K. Liu, C. H. Chen, H.-W. Wang, and S.-C. Lin, "The performance of an inspection system for indium tin oxide circuits by using a PDLC/ITO film," Proc. of SPIE, 8916, 89161N1-89161N12 (2013).
14. J.-H. Lee, T.-H. Yoon, and E-J. Choi, "Unusual temperature dependence of the splay elastic constant of a rodlike nematic liquid crystal doped with a highly kinked bent-core molecule," Phys. Rev. E, **88**, 062511 (2013).
15. A. K. Srivastava, D.-Y. Kim, J. Kim, J. Jeong, J.-H. Lee, K.-U. Jeong, and V. Singh, "Dielectric relaxation in a novel tapered chiral photochromatic liquid crystalline dendrimer," Liq. Cryst. **43**, 920-927 (2016).
16. S. O. Kasap, Principles of Electronic Materials and Devices, (McGraw Hill, 3rd Edition, 2006) Chap. 7.
17. R. Yamaguchi and S. Sato, "Relationship between film thickness and electro-optical properties in polymer dispersed liquid crystal films," Jpn. J. Appl. Phys. **33**, 4007-4011 (1994).
18. S.-H. Yoo, M.-K. Park, J.-S. Park, and H.-R. Kim, "Enhanced adhesion and transmittance uniformity in laminated polymer-dispersed liquid crystal films," J. Opt. Soc. Kor. **18**, 753-761 (2014).
19. J. Heo, T.-H. Choi, J.-W. Huh, and T.-H. Yoon, "Negative liquid crystal cell with parallel patterned electrodes for high transmittance and fast switching," J. Opt. Soc. Kor. **19**, 260-264 (2015).